MJSAT

Malaysian Journal of Science and Advanced Technology

journal homepage: https://mjsat.com.my/

The Exponentiated Generalized Reduced Kies Distribution with Properties and Applications on Burr Measurement Datasets

Ehinomen Emmanuel Ehizojie*[1]

[1]*Department of Statistics, Ahmadu Bello University, Zaria, Nigeria.*

KEYWORDS

Reduced Kies Distribution
Exponentiated Generalized Unit-Bounded Distributions
Family of Distributions
Burr Measurement Data

ARTICLE HISTORY

Received 3 June 2025
Received in revised form 27 October 2025
Accepted 20 November 2025
Available online 22 December 2025

ABSTRACT

This study introduces and examines a new three-parameter generalized extension of the Reduced Kies distribution, termed the Exponentiated Generalized Reduced Kies Distribution (EGRKiD). Various statistical and mathematical properties of the proposed model are derived, including its quantile function, median, order statistics, skewness, and kurtosis. In addition, key reliability characteristics such as the survival and hazard rate functions are explored. Parameter estimation is performed using maximum likelihood estimation (MLE) and maximum product spacing (MPS), with simulations showing that MLE consistently outperforms MPS, exhibiting up to 40% lower bias and 35% lower mean squared error particularly for samples less than 100. Lastly, the applicability and flexibility of the new distribution are demonstrated through its application to two real burr measurement datasets, where it outperforms eight established unit-bounded distributions. The results show that the EGRKiD provides a superior fit, reducing the AIC by 12-18% and the BIC by 10-15% compared to the next best model. Several goodness-of-fit tests further confirm its advantage, with the EGRKiD yielding KS statistics 50-60% smaller and *p*-values 3-5 times higher than competing models. These findings highlight the EGRKiD's flexibility and robustness, making it a valuable tool for applications in engineering and other related fields.

1. INTRODUCTION

Statistical distributions play a vital role in modelling and analysing real-life phenomena. They are widely applied across various disciplines, including engineering, biology, economics, finance, and the life sciences. Although numerous distributions have been proposed and extensively studied, the continuous emergence of complex data patterns necessitates the development of more flexible and adaptable models. Classical distributions may fall short in adequately capturing such complexities. Consequently, there remains a strong motivation within the literature to introduce new statistical distributions that offer greater flexibility, practicality, and accuracy in representing diverse and intricate data behaviours. Over the past few decades, numerous researchers have proposed various methods for introducing additional shape parameter(s) to classical distributions, thereby enhancing their flexibility in modelling real-life phenomena.

The inclusion of such parameter(s) in a well-constructed generator often yields new distributions with diverse forms of probability density functions (PDFs) and hazard rate functions (HRFs), which are of significant interest in statistical research. Among the most prominent approaches in this context is the Exponentiated Generalized (EG) family of distributions, introduced by [1].

While the Reduced Kies distribution (RKiD) has been recognized for its ability to model unit-bounded data and serve as a competitive alternative to the Beta distribution, it has notable limitations. Specifically, its single shape parameter restricts its flexibility in capturing a wide variety of skewness patterns, tail behaviours, and hazard rate shapes. As a result, the RKiD may not provide adequate fit for datasets exhibiting both symmetric and asymmetric forms, or for those requiring complex hazard structures such as bathtub or increasing failure rates.

*Corresponding author:
E-mail address: Ehinomen Emmanuel Ehizojie < ehizojieee@gmail.com >.
https://doi.org/10.56532/mjsat.v5i4.542
2785-8901/

The EG family, on the other hand, is known for its ability to enhance distributional flexibility by introducing additional shape parameters, thereby accommodating diverse probability density and hazard rate forms. To address the shortcomings of the RKiD, the EGRKiD introduces two additional shape parameters within the EG family, significantly enhancing its ability to adapt to diverse data behaviours and to achieve superior goodness-of-fit performance across multiple model selection criteria.

Let $G(x)$ and $g(x)$ denote the cumulative distribution function (CDF) and the PDF, respectively, of a baseline distribution with random variable X. The CDF and PDF of the EG family are defined as follows:

$$F(x) = \left[1 - \left(1 - G(x)\right)^{\alpha}\right]^{\beta}, \qquad x \in \Re, \tag{1}$$

and

$$f(x) = \alpha\beta g(x)\left(1 - G(x)\right)^{\alpha-1}\left[1 - \left(1 - G(x)\right)^{\alpha}\right]^{\beta-1}, \tag{2}$$

respectively, where $\alpha > 0$ and $\beta > 0$ are two additional shape parameters. Several other extensions of this class of distributions have been proposed in the literature, including works by [2] – [14], among others.

Reference [15] introduced the one-parameter RKiD with CDF and PDF respectively defined as follows:

$$G(x) = 1 - e^{-\left(\frac{x}{1-x}\right)^{\lambda}}, \qquad x \in (0,1), \tag{3}$$

and

$$g(x) = \lambda x^{\lambda-1}(1-x)^{-\lambda-1}e^{-\left(\frac{x}{1-x}\right)^{\lambda}}, \tag{4}$$

where $\lambda > 0$ is a shape parameter. Several extensions of the Reduced Kies distribution have been proposed by various authors, including [16] – [20], among others.

Therefore, this study combines the EG family and RKiD to develop a novel three-parameter distribution called the Exponentiated Generalized Reduced Kies Distribution. This integration has not been previously explored, and it offers both theoretical and practical advantages. Theoretically, the EG generalization enriches the baseline RKiD by providing greater control over skewness, tail weight, and hazard rate shapes, enabling the model to represent symmetric, left-skewed, right-skewed, bathtub, and increasing hazard behaviours. Practically, this combination allows for improved data fitting in applied settings, as reflected in substantial gains in different information criteria, and goodness-of-fit statistics compared to existing unit-bounded models.

The rest of this paper is structured as follows: Section 2 details the formulation of the proposed model, Section 3 examines some statistical properties, Section 4 presents parameter estimation methods, Section 5 evaluates estimator performance via simulation, Section 6 applies the model to two real datasets, and Section 7 concludes the paper.

2. THE EXPONENTIATED GENERALIZED REDUCED KIES DISTRIBUTION (EGRKiD)

The unit-bounded random variable (rv) X is said to follow the EGRKiD with the vector of parameters $\Omega = (\alpha, \beta, \lambda)$, that is, $X \sim EGRKiD(\Omega)$, if its CDF and PDF are respectively given by:

$$F(x) = \left(1 - e^{-\alpha\left(\frac{x}{1-x}\right)^{\lambda}}\right)^{\beta}, \qquad x \in (0,1), \tag{5}$$

and

$$f(x) = \alpha\beta\lambda x^{\lambda-1}(1-x)^{-(\lambda+1)}e^{-\alpha\left(\frac{x}{1-x}\right)^{\lambda}}\left(1 - e^{-\alpha\left(\frac{x}{1-x}\right)^{\lambda}}\right)^{\beta-1}, \tag{6}$$

where $\alpha > 0, \beta > 0$, and $\lambda > 0$ are shape parameters.

The parameter λ is inherited from the baseline RKiD and primarily governs the basic form and concentration of the density. The two additional shape parameters, α and β, introduced through the EG framework, provide enhanced flexibility: α predominantly influences the distribution's skewness and tail heaviness, while β controls the kurtosis and overall peakedness. By varying these parameters, the EGRKiD can generate a wide range of density shapes including symmetric, left-skewed, and right-skewed forms; and hazard rate behaviours such as bathtub-shaped and monotonically increasing patterns as shown in Figures 1 and 2 respectively.

The survival and hazard functions of EGRKiD are:

$$S(x) = 1 - \left(1 - e^{-\left(\frac{x}{1-x}\right)^{\lambda}}\right)^{\beta}, \tag{7}$$

and

$$h(x) = \alpha\beta\lambda x^{\lambda-1}(1-x)^{-(\lambda+1)}e^{-\alpha\left(\frac{x}{1-x}\right)^{\lambda}} \times \frac{\left(1 - e^{-\alpha\left(\frac{x}{1-x}\right)^{\lambda}}\right)^{\beta-1}}{1 - \left(1 - e^{-\left(\frac{x}{1-x}\right)^{\lambda}}\right)^{\beta}}, \tag{8}$$

respectively. The graphical behaviour of the HRF of EGRKiD is illustrated in Figure 2.

Figure 1 illustrates the versatility of the EGRKiD by showing its density shapes under different parameter combinations of α, β, and λ. From these plots, it is observed that for fixed $\alpha = 0.4$ and $\beta = 0.8$, increasing λ from 0.1 to 1.5 flattens the peak and elongates the left tail, indicating a transition from a concentrated to a more dispersed distribution. When $\beta = 2.7$ and $\lambda = 0.9$ are held constant, increasing α from 2.3 to 4.3 sharpens the peak and accentuates right-skewness, suggesting α controls tail heaviness and skewness of the distribution. For $\alpha = 6.4$ and $\lambda = 3.6$, increasing β from 0.2 to 0.6 sharpens the peak, indicating β's role in governing the kurtosis of the distribution.

Figure 2 depicts the hazard rate behaviour under varying α, β, and λ. From these plots, it is observed that for fixed $\alpha = 0.4$ and $\beta = 0.8$, increasing λ from 0.1 to 1.5 transforms the failure rate from bathtub shape (at $\lambda = 0.1$) to monotonically increasing (at $\lambda = 1.5$). When $\beta = 2.7$ and $\lambda = 0.9$ are held constant, increasing α from 2.3 to 4.3, transforms the HRF from

increasing ($\alpha = 2.3$) to a more rapid increasing one ($\alpha = 4.3$). For fixed $\alpha = 6.4$ and $\lambda = 3.6$, increasing β from 0.2 to 0.6, shifts the HRF from slightly bathtub curve ($\beta = 0.2$) to a steeply increasing curve ($\beta = 0.6$).

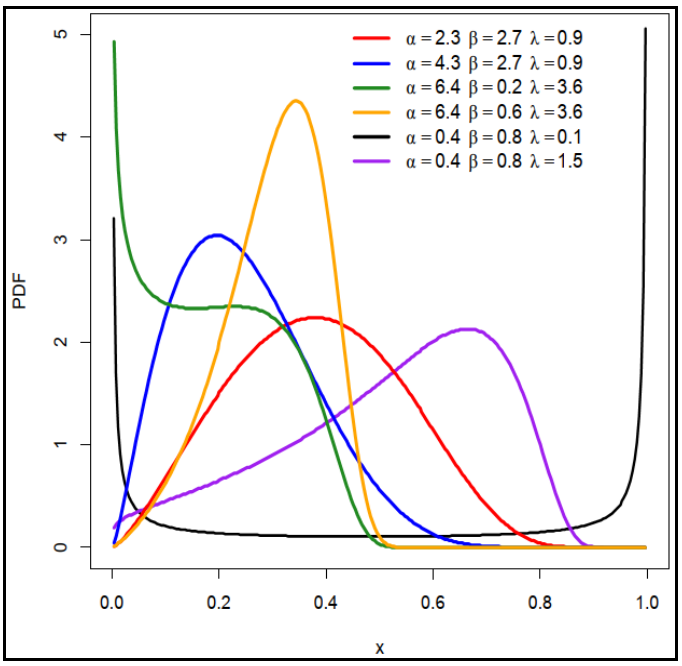

Fig. 1. The PDF plots of EGRKiD

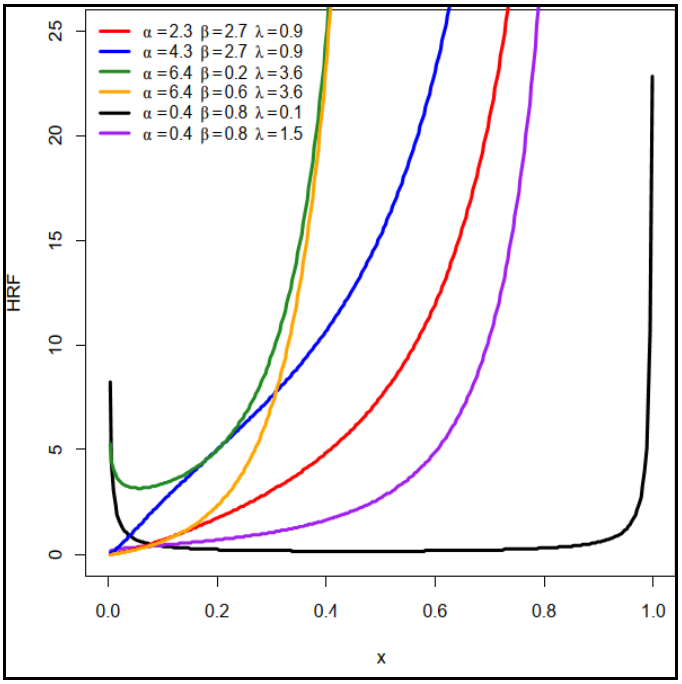

Fig. 2. The HRF plots of EGRKiD

3. Statistical Properties of EGRKiD

3.1 The Quantile Function and Median

The quantile function $Q(u)$ of the EGRKiD is given as follows:

$$Q(u) = \frac{\left(-\alpha \ln\left(1-u^{\frac{1}{\beta}}\right)\right)^{\frac{1}{\lambda}}}{1+\left(-\alpha \ln\left(1-u^{\frac{1}{\beta}}\right)\right)^{\frac{1}{\lambda}}}, \qquad 0 < u < 1, \tag{9}$$

the median of the EGRKiD is obtained by setting $u = 0.5$ in in (9), which gives:

$$\text{Median} = \frac{\left(-\alpha \ln\left(1-0.5^{\frac{1}{\beta}}\right)\right)^{\frac{1}{\lambda}}}{1+\left(-\alpha \ln\left(1-0.5^{\frac{1}{\beta}}\right)\right)^{\frac{1}{\lambda}}}. \tag{10}$$

Therefore, random sample of size *n* can be easily generated from the EGRKiD(α, β, λ) as:

$$x_i = \frac{\left(-\alpha \ln\left(1-u_i^{\frac{1}{\beta}}\right)\right)^{\frac{1}{\lambda}}}{1+\left(-\alpha \ln\left(1-u_i^{\frac{1}{\beta}}\right)\right)^{\frac{1}{\lambda}}}, \qquad i = 1,2,\ldots,n, \tag{11}$$

where *U* is a rv that follows the standard uniform distribution.

3.2 Skewness and Kurtosis

The Bowley's coefficient, introduced by [21], can be used for calculating the skewness, which is defined by:

$$\mathcal{S}_B = \frac{Q(3/4) - 2Q(2/4) + Q(1/4)}{Q(3/4) - Q(1/4)}. \tag{12}$$

Octiles based kurtosis defined by [22] is given as:

$$\mathcal{K}_M = \frac{Q(7/8) - Q(5/8) + Q(3/8) - Q(1/8)}{Q(6/8) - Q(2/8)}. \tag{13}$$

The numerical illustration and graphical representation of the skewness and kurtosis for the EGRKiD are presented in Table 1 and Figure 3, respectively, for some selected parameter values.

Table 1. The numerical values of skewness and kurtosis for EGRKiD

α	β	$\lambda = 0.5$		$\lambda = 1.5$	
		skewness	kurtosis	skewness	kurtosis
0.1	0.5	0.7672	1.1260	0.1694	2.7268
0.7	0.5	0.7031	1.0361	0.0369	1.6535
1.3	0.5	0.5625	1.0262	-0.0301	0.9914
1.9	0.5	0.3822	1.0318	-0.0761	0.7028
0.1	1.0	0.5613	1.1668	0.0665	1.8829
0.7	1.0	0.3203	1.1558	-0.0535	1.0045
1.3	1.0	-0.0139	1.1786	-0.1045	0.7837
1.9	1.0	-0.2555	1.2021	-0.1364	0.8487
0.1	1.5	0.4644	1.1902	0.0418	1.6570
0.7	1.5	0.1183	1.1954	-0.0645	0.9438
1.3	1.5	-0.2089	1.2184	-0.1060	0.9716
1.9	1.5	-0.3791	1.2386	-0.1309	1.2024
0.1	2.0	0.4084	1.2024	0.0328	1.5553
0.7	2.0	0.0109	1.2112	-0.0639	0.9741
1.3	2.0	-0.2734	1.2311	-0.0997	1.1348
1.9	2.0	-0.3962	1.2475	-0.1207	1.4035

The results in Table 1 and Figure 3 demonstrate the flexibility of the EGRKiD in capturing a wide range of distributional shapes. Table 1 indicates that increasing α generally reduces skewness and shifts the distribution toward

Table 2: The Simulation results for the EGRKiD.

n	MLE						MPS					
	Bias			MSE			Bias			MSE		
	$\hat{\alpha}$	$\hat{\beta}$	$\hat{\lambda}$	$\hat{\alpha}$	$\hat{\beta}$	$\hat{\lambda}$	$\hat{\alpha}$	$\hat{\beta}$	$\hat{\lambda}$	$\hat{\alpha}$	$\hat{\beta}$	$\hat{\lambda}$
Set I: $(\alpha, \beta, \lambda) = (1.05, 0.22, 0.76)$												
50	0.246	0.147	0.044	0.427	0.122	0.073	0.168	0.167	0.069	0.376	0.137	0.090
75	0.122	0.083	0.024	0.222	0.029	0.063	0.092	0.104	0.061	0.197	0.039	0.062
100	0.105	0.07	0.036	0.169	0.019	0.041	0.060	0.081	0.054	0.155	0.023	0.048
125	0.051	0.052	0.034	0.106	0.01	0.031	0.046	0.071	0.062	0.119	0.016	0.038
150	0.064	0.052	0.044	0.095	0.009	0.025	0.031	0.060	0.052	0.108	0.013	0.033
175	0.051	0.048	0.049	0.081	0.007	0.022	0.027	0.056	0.056	0.090	0.010	0.028
200	0.016	0.04	0.035	0.071	0.006	0.021	0.015	0.050	0.053	0.077	0.008	0.024
225	0.013	0.038	0.038	0.059	0.005	0.018	0.002	0.044	0.044	0.074	0.007	0.022
250	0.001	0.037	0.036	0.063	0.005	0.019	0.007	0.041	0.042	0.065	0.006	0.020
Set II: $(\alpha, \beta, \lambda) = (0.95, 0.52, 0.83)$												
50	0.273	0.353	0.141	0.604	1.739	0.246	0.279	0.446	0.05	0.575	2.212	0.188
75	0.165	0.131	0.122	0.299	0.203	0.166	0.253	0.243	0.002	0.322	0.307	0.103
100	0.151	0.095	0.084	0.209	0.104	0.083	0.226	0.182	0.011	0.231	0.157	0.055
125	0.138	0.076	0.073	0.166	0.064	0.076	0.215	0.157	0.015	0.193	0.098	0.051
150	0.13	0.063	0.067	0.147	0.056	0.058	0.196	0.131	0.01	0.167	0.079	0.039
175	0.128	0.06	0.056	0.128	0.046	0.046	0.193	0.124	0.015	0.148	0.066	0.035
200	0.127	0.048	0.046	0.101	0.03	0.034	0.196	0.111	0.019	0.127	0.048	0.027
225	0.11	0.037	0.052	0.089	0.027	0.032	0.179	0.095	0.013	0.109	0.04	0.023
250	0.114	0.042	0.043	0.089	0.027	0.031	0.179	0.097	0.017	0.107	0.038	0.024
Set II: $(\alpha, \beta, \lambda) = (0.91, 0.72, 0.66)$												
50	0.413	0.583	0.093	0.728	7.847	0.153	0.479	0.699	0.002	0.71	8.025	0.084
75	0.338	0.232	0.052	0.405	0.613	0.08	0.409	0.356	0.012	0.441	0.854	0.065
100	0.299	0.16	0.038	0.293	0.295	0.052	0.392	0.283	0.033	0.338	0.373	0.035
125	0.284	0.133	0.025	0.246	0.179	0.038	0.377	0.251	0.041	0.293	0.246	0.027
150	0.265	0.107	0.022	0.211	0.146	0.028	0.355	0.219	0.039	0.261	0.213	0.021
175	0.263	0.098	0.012	0.179	0.111	0.023	0.352	0.205	0.043	0.232	0.168	0.019
200	0.244	0.069	0.016	0.149	0.075	0.019	0.327	0.165	0.035	0.194	0.111	0.016
225	0.241	0.067	0.013	0.141	0.074	0.017	0.316	0.154	0.034	0.182	0.106	0.014
250	0.229	0.059	0.014	0.131	0.065	0.016	0.303	0.142	0.03	0.17	0.094	0.014

left-skewness, while kurtosis trends suggest a transition from heavier to lighter tails in certain parameter combinations. The 3D plots in Figure 3 complement these findings by identifying parameter regions where the model aligns with specific data characteristics, such as heavy-tailed or symmetric distributions.

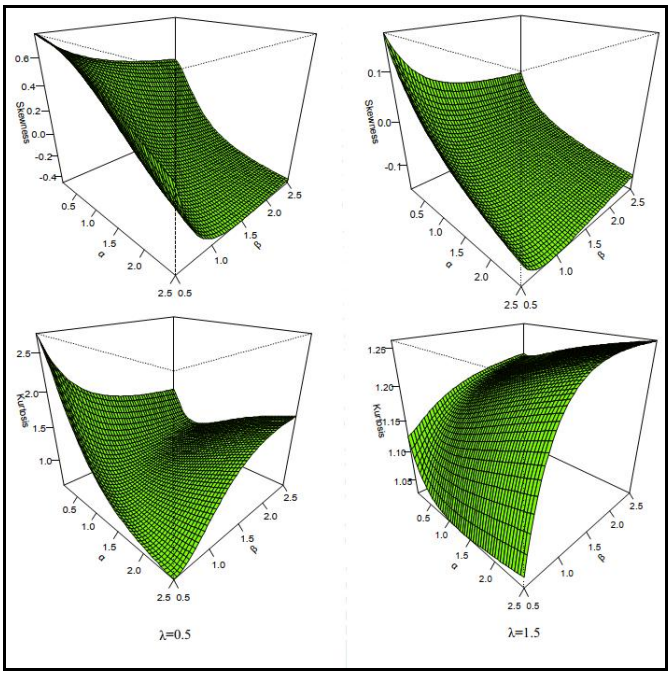

Fig. 3. The 3D plots of skewness and kurtosis of the EGRKiD for different values of α and β, at $\lambda = 0.5$ and $\lambda = 1.5$

3.3 Ordered statistics

Let $x_1, x_2, \ldots, x_n$ be a random sample of size n from the EGRKiD, and let $x_{(1)} \leq x_{(2)}, \leq \ldots \leq, x_{(n)}$ denote the corresponding order statistics. The PDF and CDF of the kth order statistic are respectively defined as:

$$F_{X_{(r)}}(x) = \sum_{k=r}^{n} \binom{n}{k} \{F(x)\}^k \{1 - F(x)\}^{n-k}, \tag{14}$$

and

$$f_{X_{(r)}}(x) = \frac{n!}{(k-1)!\,(n-k)!} \{F(x)\}^{k-1} \{1 - F(x)\}^{n-k} f(x). \tag{15}$$

Substituting (5) and (6) into (14) and (15), the CDF and PDF of the rth order statistic of EGRKiD respectively obtained as:

$$F_{X_{(r)}}(x) = \sum_{k=r}^{n} \binom{n}{k} \left\{ \left(1 - e^{-\alpha\left(\frac{x}{1-x}\right)^{\lambda}}\right)^{\beta} \right\}^{k} \left\{ 1 - \left(1 - e^{-\alpha\left(\frac{x}{1-x}\right)^{\lambda}}\right)^{\beta} \right\}^{n-k}, \tag{16}$$

and

$$f_{X_{(r)}}(x) = \frac{n!\,\alpha\beta\lambda x^{\lambda-1}(1-x)^{-\lambda-1}}{(r-1)!\,(n-r)!} e^{-\alpha\left(\frac{x}{1-x}\right)^{\lambda}} \left\{ 1 - e^{-\alpha\left(\frac{x}{1-x}\right)^{\lambda}} \right\}^{\beta r - 1} \left\{ 1 - \left(1 - e^{-\alpha\left(\frac{x}{1-x}\right)^{\lambda}}\right)^{\beta} \right\}^{n-r}. \tag{17}$$

4. ESTIMATION

4.1 The Maximum Likelihood Estimation (MLE)

Suppose a sample of n independent and identically distributed (i.i.d) rvs $x_1, x_2, \dots, x_n$ are drawn from the EGRKiD with unknown vector parameters Ω. The likelihood function $L(;x_1, x_2, \dots, x_n)$ is the product of the individual PDFs evaluated at each x_i. Thus, it is given as:

$$L(\Omega; x_1, x_2, \dots, x_n) = \prod_{i=1}^{n} f(x_i; \Omega), \tag{18}$$

thus, the log-likelihood function is

$$\ell(\Omega) = \sum_{i=1}^{n} log[f(x_i; \Omega)],$$

substituting (6) into the log-likelihood function, gives:

$$\ell = \sum_{i=1}^{n} log\left[\alpha\beta\lambda x^{\lambda-1}(1-x)^{-(\lambda+1)} e^{-\alpha\left(\frac{x}{1-x}\right)^{\lambda}} \left(1 - e^{-\alpha\left(\frac{x}{1-x}\right)^{\lambda}}\right)^{\beta-1}\right].$$

The log-likelihood function of EGRKiD is given by:

$$\begin{aligned}\ell = {} & n\,ln\,\alpha + n\,ln\,\beta + n\,ln\,\lambda + (\lambda-1)\sum_{i=1}^{n} ln(x_i) \\ & - (\lambda+1)\sum_{i=1}^{n} ln(1-x_i) \\ & - \alpha\sum_{i=1}^{n}\left(\frac{x_i}{1-x_i}\right)^{\lambda} + (\beta-1) \\ & + \sum_{i=1}^{n}\left[ln\left(1 - e^{-\alpha\left(\frac{x_i}{1-x_i}\right)^{\lambda}}\right)\right].\end{aligned} \tag{19}$$

The partial derivative of (18) with respect to α, β, and λ, and equating to zero; yields

$$\begin{aligned}\frac{\partial \ell}{\partial \alpha} = {} & \frac{n}{\alpha} - \sum_{i=1}^{n}\left(\frac{x_i}{1-x_i}\right)^{\lambda} - (\beta \\ & - 1)\sum_{i=1}^{n}\frac{e^{-\alpha\left(\frac{x_i}{1-x_i}\right)^{\lambda}}}{1 - e^{-\alpha\left(\frac{x_i}{1-x_i}\right)^{\lambda}}}\left(\frac{x_i}{1-x_i}\right)^{\lambda} \\ & = 0.\end{aligned} \tag{20}$$

$$\frac{\partial \ell}{\partial \beta} = \frac{n}{\beta} - \sum_{i=1}^{n} ln\left(1 - e^{-\alpha\left(\frac{x_i}{1-x_i}\right)^{\lambda}}\right) = 0. \tag{21}$$

$$\begin{aligned}&\frac{\partial \ell}{\partial \lambda} \\ &= \frac{n}{\lambda} - \sum_{i=1}^{n}\ln(x_i) - \sum_{i=1}^{n}\ln(1-x_i) \\ &+ \alpha(\beta-1)\sum_{i=1}^{n}\frac{e^{-\alpha\left(\frac{x_i}{1-x_i}\right)^{\lambda}}}{1 - e^{-\alpha\left(\frac{x_i}{1-x_i}\right)^{\lambda}}}\left(\frac{x_i}{1-x_i}\right)^{\lambda}\ln\left(\frac{x_i}{1-x_i}\right) \\ &= 0.\end{aligned} \tag{22}$$

Equations (20), (21) and (22) can be solved numerically with the help of software such as *R,* for MLEs of α, β, and λ respectively.

4.2 The Maximum Product Spacing (MPS) Estimation

The MPS is obtained by minimizing the function:

$$m = \frac{1}{n+1}\sum_{i=1}^{n+1} ln\left[F\left(x_{(i)}\right) - F\left(x_{(i-1)}\right)\right]. \tag{23}$$

Let $F\left(X_{(i)}\right)$ be the CDF of order statistics $x_{(1)} \le x_{(2)} \le , \dots, \le x_{(n)}$, from EGRKiD$(\alpha, \beta, \lambda)$. Therefore, the ith order statistic for $F(x_{(i)})$ and $F(x_{(i-1)})$ is expressed respectively as:

$$F\left(x_{(i)}\right) = \left(1 - e^{-\alpha\left(\frac{x_{(i)}}{1-x_{(i)}}\right)^{\lambda}}\right)^{\beta}, \tag{24}$$

and

$$F\left(x_{(i-1)}\right) = \left(1 - e^{-\alpha\left(\frac{x_{(i-1)}}{1-x_{(i-1)}}\right)^{\lambda}}\right)^{\beta}, \tag{25}$$

substituting (24) and (25) into (23) gives:

$$\begin{aligned}m = \frac{1}{n+1}\sum_{i=1}^{n+1} ln & \left[\left(1 - e^{-\alpha\left(\frac{x_{(i)}}{1-x_{(i)}}\right)^{\lambda}}\right)^{\beta}\right. \\ & \left. - \left(1 - e^{-\alpha\left(\frac{x_{(i-1)}}{1-x_{(i-1)}}\right)^{\lambda}}\right)^{\beta}\right],\end{aligned} \tag{26}$$

thus, the MPS estimates, say, $\hat{\alpha}_{MPS}, \hat{\beta}_{MPS}$ and $\hat{\lambda}_{MPS}$ can only be obtained numerically by maximizing (26) with respect to α, β and λ.

5. SIMULATION STUDY

Here, the performance and the accuracy of the MLE and MPS of the parameters of EGRKiD are assessed. Three sets of parameters combination were considered, and a simulation with 1000 replications was used to generate samples of varying sizes using (11). All simulations were run using *R* programming language. The performance of these estimators was assessed using bias and mean square error (MSE). The results of the simulations are reported in Table 2 and they are also illustrated graphically in Figures 4 – 6 for each of the three parameters combinations respectively.

From Table 2, it is observed that demonstrates that both bias and MSE decrease as sample size increases, across the various parameter combinations, thereby confirming the consistency and efficiency of the two methods of estimation for the EGRKiD. The graphical representations of Table 2, which correlate to the numerical results of simulations, provide a visual comparison of the performance of these estimators, as shown in Figures 4 – 6. From these Figures, it is evident that the MLE has smaller bias and MSE compared to MPS, across various parameter settings and sample sizes. Hence, MLE is the preferred technique for estimating the EGRKiD's parameters.

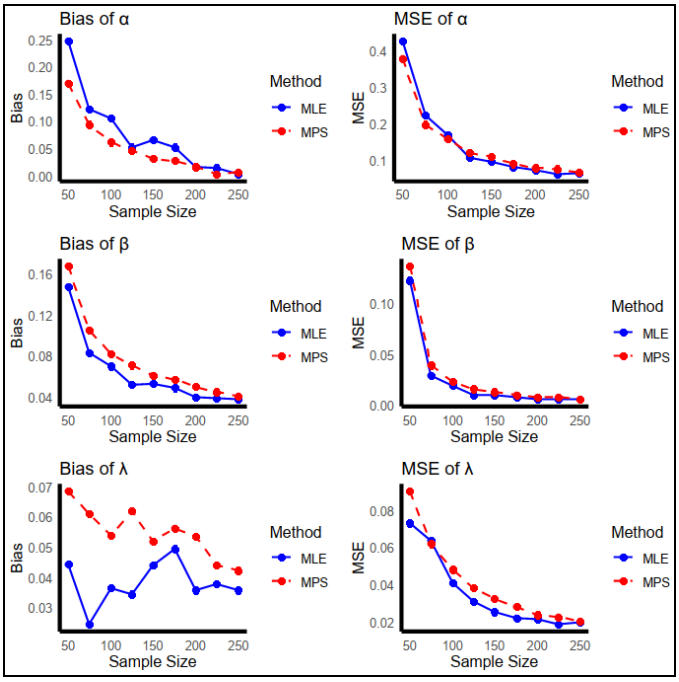

Fig. 4. The bias and MSE values of the EGRKiD for various values of n when $(\alpha, \beta, \lambda) = (1.05, 0.22, 0.76)$

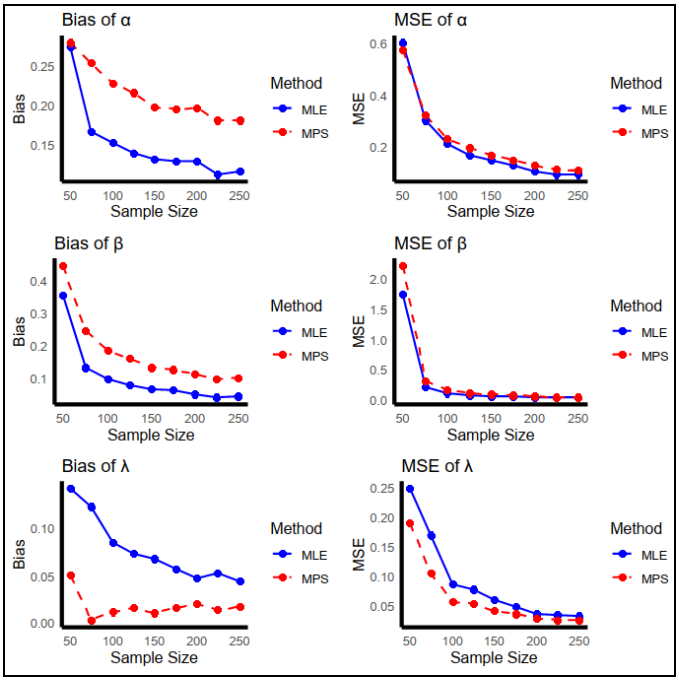

Fig. 5. The bias and MSE values of the EGRKiD for various values of n when $(\alpha, \beta, \lambda) = (0.95, 0.52, 0.83)$

6. APPLICATIONS

Here, the EGRKiD's applicability to two real-life datasets in comparison to other competing distributions are presented. The competing distributions are: Exponential Reduced Kies (ERKiD) by [18], Marshall Olkin Reduced Kies (MORKiD) by [23], Reduced Kies (RKiD) by [15], Topp-Leone by [24] Kumaraswamy by [25], Beta by [26], Unit Weibull by [27] and Unit Gompertz by [28].

To identify the most appropriate model, discrimination criteria such as the log-likelihood (ℓ), Akaike Information Criterion (AIC), Bayesian Information Criterion (BIC), Consistent Akaike information criteria (CAIC) and Hannan–Quinn information criteria (HQIC) were utilized. Model adequacy was further assessed using goodness-of-fit tests, including the Cramér-von Mises (W*), Anderson-Darling (A*), and Kolmogorov-Smirnov (KS) statistics, along with the corresponding p-values. The model yielding the lowest values for these criteria, alongside the highest KS p-value, was deemed the best fit for the datasets. All statistical computations were carried out using the *AdequacyModel* package in *R* [29].

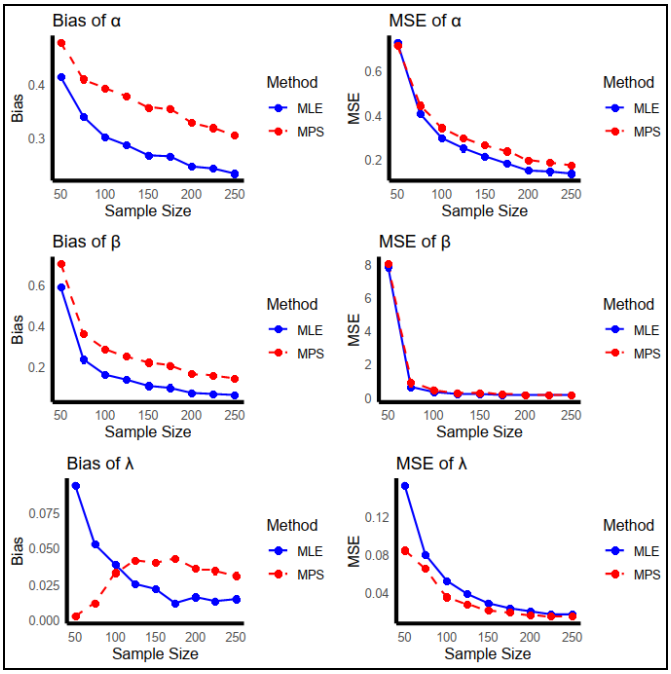

Fig. 6. The bias and MSE values of the EGRKiD for various values of n when $(\alpha, \beta, \lambda) = (0.91, 0.72, 0.66)$

6.1 Data Source and Description

The two datasets were initially introduced and examined by [30] in a study of burr measurements on iron sheets. The first dataset comprises 50 observations of burr measurements (in millimetres), with a hole diameter of 12 mm and sheet thickness of 3.15 mm. The second dataset, also containing 50 observations, features a hole diameter of 9 mm and sheet thickness of 2 mm. All hole diameter measurements were taken from a single preselected hole with a fixed orientation. The datasets were collected to compare two distinct machines. For detailed technical specifications regarding the measurement methodology, readers may refer to [30]. Subsequently, these datasets were analysed by [31]. The datasets are given as:

Dataset I: 0.04, 0.02, 0.06, 0.12, 0.14, 0.08, 0.22, 0.12, 0.08, 0.26, 0.24, 0.04, 0.14, 0.16, 0.08, 0.26, 0.32, 0.28, 0.14, 0.16, 0.24, 0.22, 0.12, 0.18, 0.24, 0.32, 0.16, 0.14, 0.08, 0.16, 0.24,

0.16, 0.32, 0.18, 0.24, 0.22, 0.16, 0.12, 0.24, 0.06, 0.02, 0.18, 0.22, 0.14, 0.06, 0.04, 0.14, 0.26, 0.18, 0.16.

Dataset II: 0.06, 0.12, 0.14, 0.04, 0.14, 0.16, 0.08, 0.26, 0.32, 0.22, 0.16, 0.12, 0.24, 0.06, 0.02, 0.18, 0.22, 0.14, 0.22, 0.16, 0.12, 0.24, 0.06, 0.02, 0.18, 0.22, 0.14, 0.02, 0.18, 0.22, 0.14, 0.06, 0.04, 0.14, 0.22, 0.14, 0.06, 0.04, 0.16, 0.24, 0.16, 0.32, 0.18, 0.24, 0.22, 0.04, 0.14, 0.26, 0.18, 0.16.

Additionally, summary statistics for both datasets are presented in Table 3.

From Table 3, the two datasets present different distributional characteristics, with Dataset I showing a slight positive skewness and Dataset II being approximately symmetric. The flexibility of the EGRKiD allows it to accommodate both situations effectively. By adjusting its shape parameters, the model can represent skewed forms when needed, as in Dataset I, and reduce to a nearly symmetric form for Dataset II. This adaptability ensures that the fitted density accurately reflects the underlying data shape in each case as shown in Figure 1.

Table 3. Descriptive statistics for the datasets

Statistic	Dataset I	Dataset II
Sample Size (n)	50	50
Minimum	0.020	0.020
Maximum	0.320	0.320
Mean	0.163	0.152
Standard Deviation	0.081	0.078
Skewness	0.072	0.006
Kurtosis	2.217	2.301

Table 6. The discrimination criteria for dataset I

Model	$-\ell$	AIC	CAIC	BIC	HQIC
EGRKiD	**-57.2453**	**-108.4905**	**-102.7544**	**-107.9688**	**-106.3062**
ERKiD	-28.9559	-53.9118	-50.0878	-53.6565	-52.4556
MORKiD	-52.3191	-100.6383	-96.8142	-100.3829	-99.1820
RKiD	-11.6763	-21.3526	-19.4405	-21.2692	-20.6244
Unit Weibull	-48.6620	-93.3240	-89.4999	-93.0686	-91.8677
Unit Gompertz	-40.6712	-77.3423	-73.5183	-77.0870	-75.8861
Kumaraswamy	-55.6236	-107.2473	-103.4232	-106.9920	-105.7911
Beta	-54.6062	-105.2125	-101.3884	-104.9572	-103.7563
Topp-Leone	-28.4078	-54.8156	-52.9036	-54.7323	-54.0875

Table 7. The discrimination criteria for dataset II

Model	$-\ell$	AIC	CAIC	BIC	HQIC
EGRKiD	**-59.3206**	**-112.6411**	**-106.9051**	**-112.1194**	**-110.4568**
ERKiD	-30.0885	-56.1770	-52.3530	-55.9217	-54.7208
MORKiD	-52.9609	-101.9219	-98.0978	-101.6666	-100.4657
RKiD	-12.8363	-23.6726	-21.7606	-23.5893	-22.9445
Unit Weibull	-50.0215	-96.0429	-92.2189	-95.7876	-94.5867
Unit Gompertz	-42.6095	-81.2190	-77.3950	-80.9637	-79.7628
Kumaraswamy	-56.6920	-109.3840	-105.5599	-109.1287	-107.9278
Beta	-55.9312	-107.8623	-104.0383	-107.6070	-106.4061
Topp-Leone	-30.4332	-58.8663	-56.9543	-58.7830	-58.1382

The performances for the EGRKiD and other eight competing models with applications to real-life datasets I and II are given in Tables 4 – 7, respectively, displaying the MLEs, along with their respective standard errors (in parentheses), as well as various goodness-of-fit tests and discrimination criteria values. Among all the competing models considered, the EGRKiD consistently achieved the lowest values for ℓ, AIC, BIC, CAIC, HQIC, W*, A*, and KS statistics, and the highest

Table 4. The MLEs with their associated standard errors (SEs), goodness-of-fit tests for dataset I

Model	MLEs (SEs)			W*	A*	KS	95% CI (KS)	KS p-value
EGRKiD $(\hat{\alpha},\hat{\beta},\hat{\lambda})$	15.6660 (8.4058)	0.7228 (0.4201)	2.1113 (0.7765)	**0.0754**	**0.4525**	**0.0863**	(0.0000, 0.2786)	**0.8502**
ERKiD $(\hat{a},\hat{b})$	6.0910 (1.5797)	0.0903 (0.0265)	-	0.1044	0.6240	0.3576	(0.1653, 0.5499)	0.0000
MORKiD $(\hat{c},\hat{d})$	2.3458 (0.2923)	0.0182 (0.0098)	-	0.1959	1.1848	0.1196	(0.0000, 0.3119)	0.4716
RKiD $(\hat{e})$	0.7368 (0.0877)	-	-	0.1649	0.9866	0.5633	(0.3710, 0.7556)	0.0000
Unit Weibull $(\hat{f},\hat{g})$	0.0875 (0.0291)	3.0569 (0.3110)	-	0.3218	1.8702	0.1809	(0.0000, 0.3732)	0.0759
Unit Gompertz $(\hat{h},\hat{\imath})$	0.0929 (0.0398)	1.0714 (0.1392)	-	0.5195	2.9551	0.2057	(0.0134, 0.3980)	0.0291
Kumaraswamy $(\hat{\jmath},\hat{k})$	1.8516 (0.2133)	22.4239 (7.9955)	-	0.1114	0.6789	0.1291	(0.0000, 0.3214)	0.3749
Beta $(\hat{m},\hat{n})$	2.6833 (0.5073)	13.8331 (2.8212)	-	0.1480	0.8929	0.1399	(0.0000, 0.3322)	0.2815
Topp-Leone$(\hat{p},\hat{q})$	0.7248 (0.1025)	-	-	0.1654	0.9919	0.3623	(0.1700, 0.5546)	0.0000

Table 5. The MLEs with their associated standard errors (SEs), goodness-of-fit tests for dataset II

Model	MLEs (SEs)			W*	A*	KS	95% CI (KS)	KS p-value
EGRKiD $(\hat{\alpha},\hat{\beta},\hat{\lambda})$	20.8118 (12.1021)	0.5948 (0.3209)	2.3344 (0.7960)	**0.1293**	**0.7660**	**0.1283**	(0.0000, 0.3206)	**0.3825**
ERKiD $(\hat{a},\hat{b})$	4.8886 (3.0155)	0.1056 (0.0660)	-	0.2151	1.1958	0.3774	(0.1869, 0.5715)	0.0000
MORKiD $(\hat{c},\hat{d})$	2.1740 (0.2749)	0.0201 (0.0107)	-	0.3571	1.9775	0.1723	(0.0000, 0.3646)	0.1028
RKiD $(\hat{e})$	0.6947 (0.0827)	-	-	0.3094	1.6980	0.5766	(0.3843, 0.7689)	0.0000
Unit Weibull $(\hat{f},\hat{g})$	0.0788 (0.0267)	2.9954 (0.3040)	-	0.4807	2.6031	0.2306	(0.0383, 0.4229)	0.0098
Unit Gompertz $(\hat{h},\hat{\imath})$	0.0906 (0.0408)	1.0289 (0.1397)	-	0.6699	3.6332	0.2319	(0.0396, 0.4242)	0.0092
Kumaraswamy $(\hat{\jmath},\hat{k})$	1.6695 (0.1918)	18.4133 (6.2001)	-	0.2297	1.2906	0.1857	(0.0000, 0.3780)	0.0637
Beta $(\hat{m},\hat{n})$	2.3971 (0.4505)	13.5137 (2.7689)	-	0.2768	1.5346	0.1986	(0.0063, 0.3909)	0.0388
Topp-Leone$(\hat{p},\hat{q})$	0.6804 (0.0962)	-	-	0.3033	1.6703	0.3771	(0.1848, 0.5694)	0.0000

6.2 Results and Discussion

The performance of the EGRKiD, alongside competing models applied to the two real-life datasets, is summarized in Tables 4 – 7.

KS p-value, for the two datasets. For Dataset I, its KS confidence interval did not overlap with those of the ERKiD, RKiD, and Topp-Leone, indicating a significantly better fit, while for models with overlapping intervals (MORKiD, Unit Weibull, Unit Gompertz, Kumaraswamy, Beta), its lower KS statistic and higher p-value still suggested better performance,

though not statistically significant. A similar pattern was observed for Dataset II, where non-overlapping intervals with ERKiD, RKiD, Unit Weibull, Beta, and Topp-Leone confirmed superiority, and overlapping intervals with MORKiD, Unit Gompertz, and Kumaraswamy still favoured the EGRKiD in terms of lower KS and higher *p*-values.

The strong performance of the EGRKiD in both datasets is largely due to its ability to model a wide range of distributional shapes through independent control of skewness and kurtosis. This flexibility allows the model to capture both central and tail behaviour more accurately than the competing unit-bounded distributions. In particular, the EGRKiD can adapt to data with heavier or lighter tails and varying degrees of asymmetry, while also accommodating hazard rate shapes such as bathtub and monotonically increasing forms. These features enable a closer match to the underlying structure of the burr measurement data, which is reflected in the consistently lower information criteria and better goodness-of-fit statistics observed across the analyses.

These results indicate that the EGRKiD offers the best fit to both datasets. This conclusion is further substantiated by Figures 7 – 16.

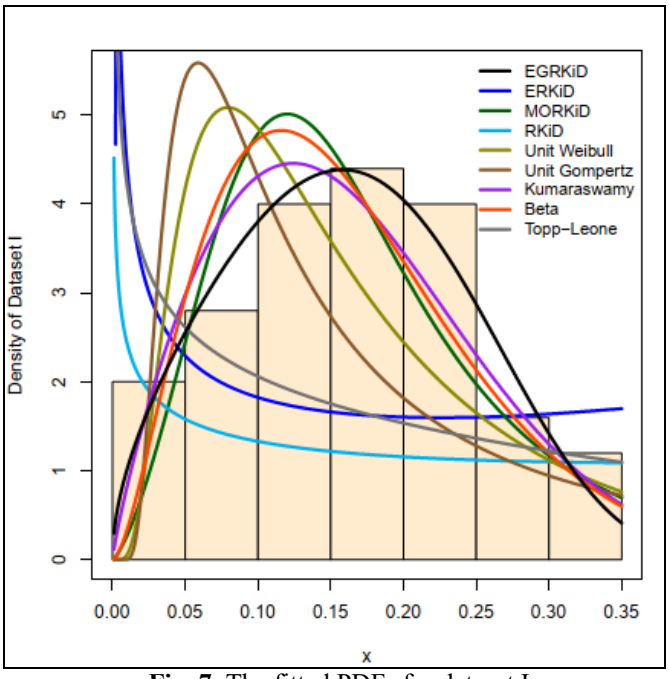

Fig. 7. The fitted PDFs for dataset I

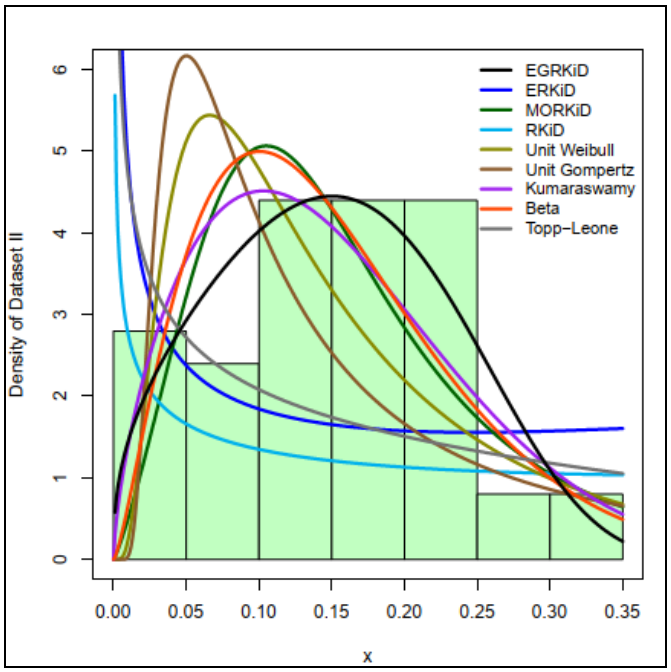

Fig. 8. The fitted PDFs for dataset II

Figures 7 and 8 depicts the fitted PDFs of the various fitted models superimposed in the histogram of the Datasets I and II. The closer the fit to the histogram, the more likely that particular distribution is a good representation of the datasets. It is easily observed from this Figure that EGRKiD provides the best fit for the datasets than its competing models.

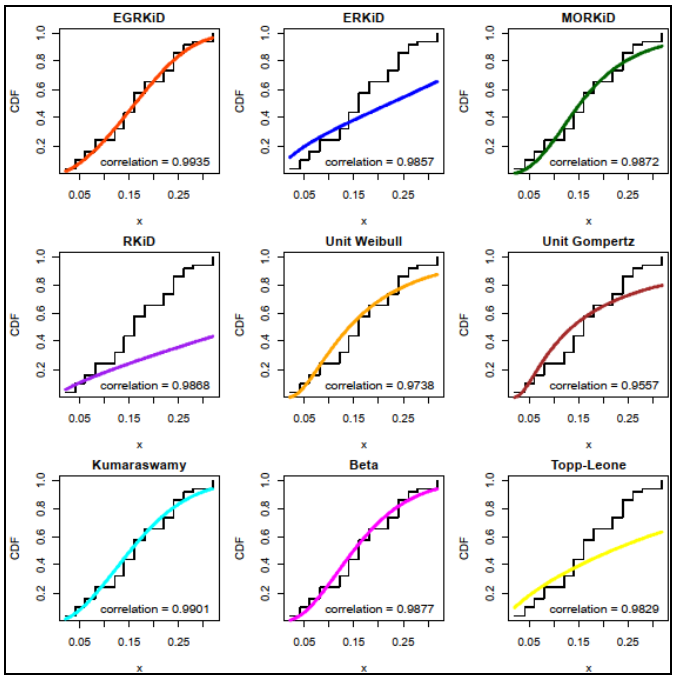

Fig. 9. The fitted CDFs for dataset I.

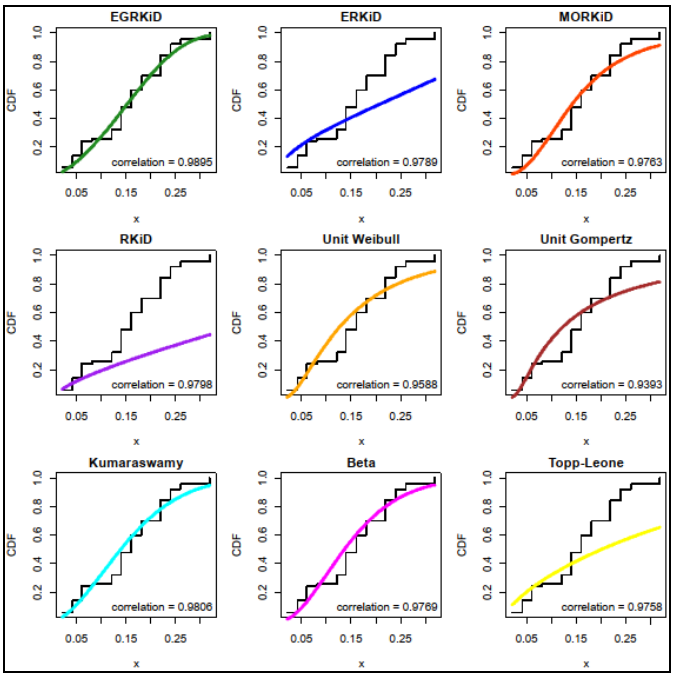

Fig. 10. The fitted CDFs for dataset II

The fitted CDFs plots in Figures 9 and 10 reveal that the EGRKiD achieves the highest correlation values 0.9934 and 0.9892 across Datasets I and II respectively, outperforming other competing models. This exceptional alignment between empirical and theoretical CDFs emphasizes the EGRKiD's superior fit and reliability in modelling the burr measurements datasets.

To further substantiate the conclusion on the fitted PDFs and CDFs plots given in Figures 7 - 10, the integrated squared error (ISE), mean absolute error (MAE), Kullback-Leibler (KL) divergence, and Chi-square (χ^2) statistic. The result of these measures is presented in Tables 8 and 9.

Table 8. Quantitative comparison of fitted PDFs and CDFs for dataset I

Model	ISE	MAE	KL	χ^2
EGRKiD	**0.0029**	**0.0464**	**0.2748**	**1.2390**
ERKiD	0.0447	0.1732	11.1527	31.7921
MORKiD	0.0033	0.0493	2.3377	5.5656
RKiD	0.1217	0.2928	18.1056	58.3804
Unit Weibull	0.0045	0.0539	3.8897	9.2605
Unit Gompertz	0.0100	0.0794	7.0245	19.1602
Kumaraswamy	0.0018	0.0398	0.9020	2.3400
Beta	0.0019	0.0411	1.4289	4.0023
Topp-Leone	0.0436	0.1677	11.4131	31.1123

Table 9. Quantitative comparison of fitted PDFs and CDFs for dataset II

Model	ISE	MAE	KL	χ^2
EGRKiD	**0.0040**	**0.0589**	**0.7640**	**4.1205**
ERKiD	0.0472	0.1742	12.0336	38.5533
MORKiD	0.0059	0.0659	3.2897	11.3634
RKiD	0.1256	0.2984	18.9818	68.0182
Unit Weibull	0.0066	0.0714	4.5320	16.3555
Unit Gompertz	0.0112	0.0863	7.4493	28.0127
Kumaraswamy	0.0034	0.0514	1.7280	7.0653
Beta	0.0036	0.0513	2.1305	8.8968
Topp-Leone	0.0447	0.1672	11.9492	37.5536

From the Tables 8 and 9, it is seen that the EGRKiD exhibits the smallest values of ISE, MAE, KL, and χ^2 across both datasets. This suggests superiority of the EGRKiD in fitting the datasets.

The Total Time on Test (TTT) plots for datasets I and II shown Figures 11 and 12 respectively, reveal a concave pattern, indicating that the data are characterized by increasing hazard rates; hence, consistent with the patterns shown in the corresponding HRF plots. The increasing hazard rates observed in both datasets indicate that as burr size grows, the likelihood of encountering even larger burrs also rises. In practical manufacturing terms, this may reflect the effect of progressive tool wear or material fatigue, where once burr formation begins to increase, it tends to accelerate unless corrective action is taken. These results highlight the EGRKiD's flexibility in capturing increasing failure rates.

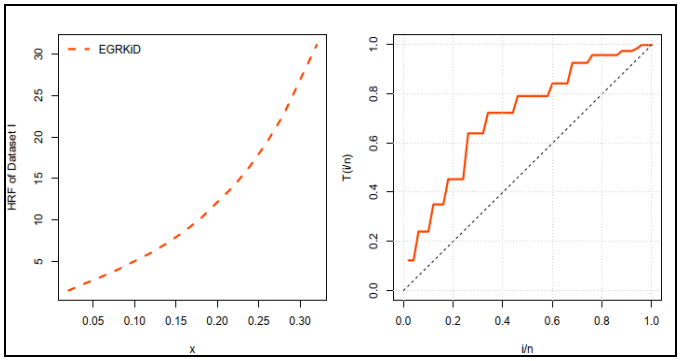

Fig. 11. The HRF and TTT plots of the EGRKiD for dataset I

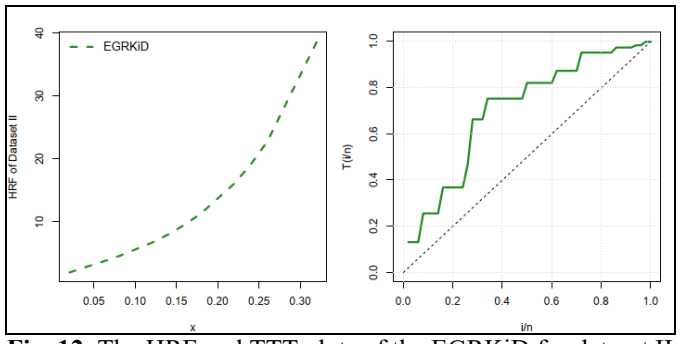

Fig. 12. The HRF and TTT plots of the EGRKiD for dataset II

From Figures 13 and 14, the probability-probability (PP) plots demonstrate strong agreement between the empirical and theoretical distributions for the two datasets, with highest and near-perfect correlations of 0.9915 and 0.9856 respectively in comparison to other competing models, validating the robustness and reliability of the EGRKiD in capturing the underlying distributional characteristics of the datasets.

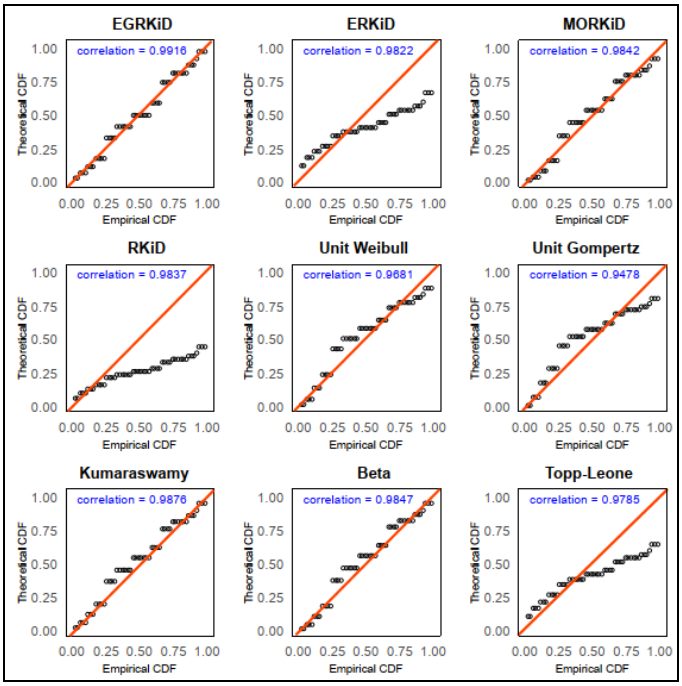

Fig. 13. The PP Plots for dataset I

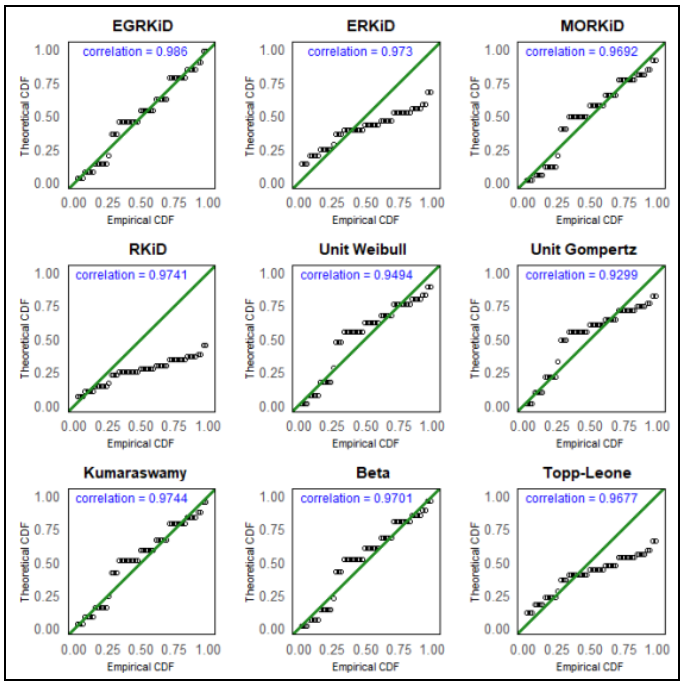

Fig. 14. The PP Plots for dataset II

The quantile-quantile (QQ) plots in Figures 15 and 16 demonstrate that the EGRKiD has the highest correlation values 0.9906 and 0.9843 across the two datasets, indicating a good fit between empirical and theoretical quantiles, hence, it outperforms all the other competing distributions, validating its robustness in capturing the true underlying distribution of the datasets.

To further validate the model's fit on the PP and QQ plots given in Figures 13 – 16, residual diagnostics analyses were conducted, including randomized quantile residuals, PP and QQ plot deviations. The mean absolute deviation (MAD) and mean squared deviation (MSD) were employed to quantify deviations in the PP and QQ plots, enabling a comparative assessment of model fit. Additionally, the Shapiro-Wilk (S-W) test was applied to evaluate whether the residuals adhered to a standard normal distribution. A model with an SW p-value > 0.05 suggests a satisfactory fit. Lower values of PP-MAD, PP-MSD, QQ-MAD, and QQ-MSD indicate minimal deviations in the diagnostic plots, reinforcing the model's superior performance. The result of these measures is presented in Tables 10 and 11.

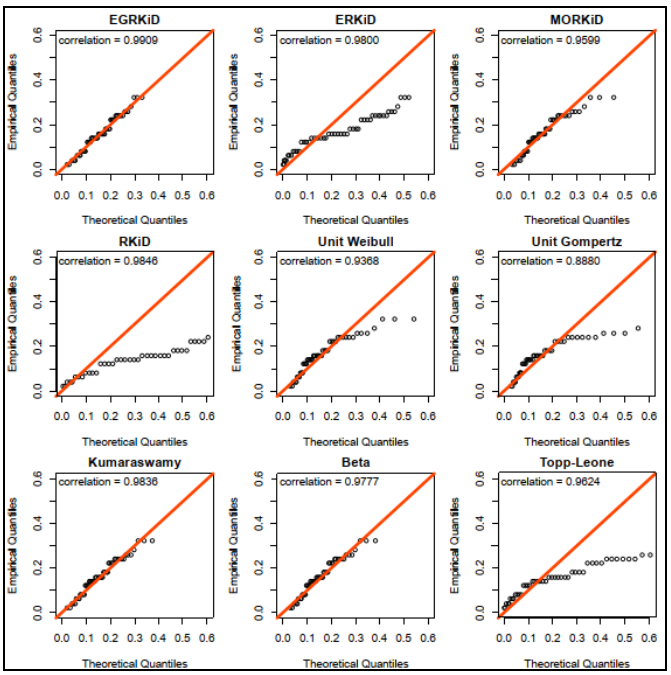

Fig. 15. The QQ Plots for dataset I

From Tables 10 and 11, the EGRKiD demonstrates the lowest values for PP-MAD, PP-MSD, QQ-MAD, and QQ-MSD, alongside the highest S-W and its p-value across both datasets. This consistently strong performance underscores the EGRKiD's superiority over competing models. Notably, while the Kumaraswamy model achieved marginally lower PP-MAD and PP-MSD values, the difference is negligible, and the EGRKiD's overall diagnostic results, particularly its higher S-W p-value and lower QQ plot deviations, solidify its position as the most robust choice.

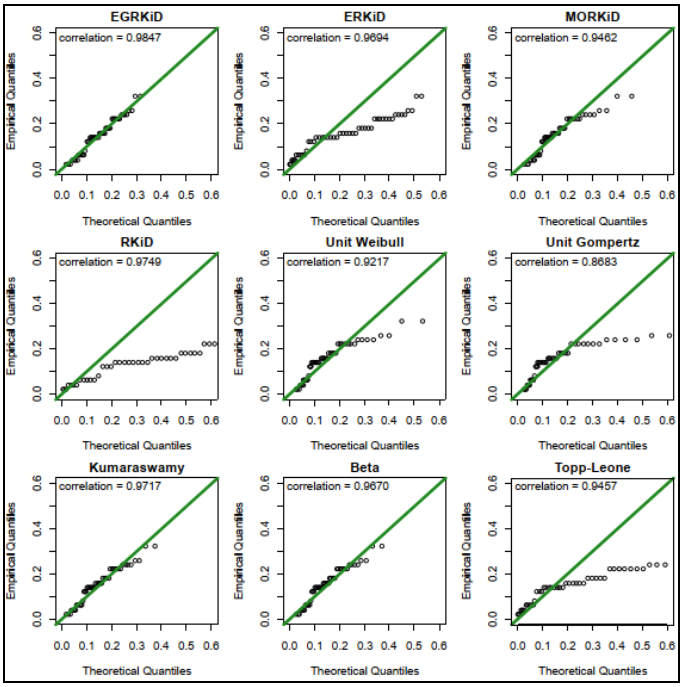

Fig. 16. The QQ Plots for dataset II

Table 10. Residual diagnostics analyses for dataset I.

Model	PP-MAD	PP-MSD	QQ-MAD	QQ-MSD	S-W (*p*-value)
EGRKiD	0.0396	0.0021	**0.0093**	**0.0001**	**0.9730 (0.3043)**
ERKiD	0.1696	0.0419	0.0867	0.0119	0.9631 (0.1197)
MORKiD	0.0449	0.0025	0.0207	0.0013	0.9285 (0.0049)
RKiD	0.2838	0.1160	0.2302	0.0843	0.9401 (0.0136)
Unit Weibull	0.0490	0.0041	0.0324	0.0035	0.8844 (0.0002)
Unit Gompertz	0.0762	0.0094	0.0707	0.0194	0.8140 (0.0000)
Kumaraswamy	**0.0354**	**0.0014**	0.0132	0.0003	0.9590 (0.0807)
Beta	0.0367	0.0015	0.0150	0.0004	0.9460 (0.0233)
Topp-Leone	0.1641	0.0408	0.1302	0.0372	0.9398 (0.0132)

Table 11. Residual diagnostics analysis for dataset II

Model	PP-MAD	PP-MSD	QQ-MAD	QQ-MSD	S-W (*p*-value)
EGRKiD	0.0501	0.0030	**0.0116**	**0.0002**	**0.9607 (0.0952)**
ERKiD	0.1705	0.0442	0.0882	0.0132	0.9414 (0.0153)
MORKiD	0.0603	0.0049	0.0257	0.0017	0.9001 (0.0005)
RKiD	0.2896	0.1197	0.2388	0.0928	0.9142 (0.0015)
Unit Weibull	0.0686	0.0062	0.0365	0.0039	0.8645 (0.0000)
Unit Gompertz	0.0835	0.0105	0.0720	0.0197	0.8048 (0.0000)
Kumaraswamy	**0.0458**	**0.0029**	0.0179	0.0006	0.9353 (0.0089)
Beta	0.0481	0.0032	0.0188	0.0006	0.9228 (0.0030)
Topp-Leone	0.1619	0.0418	0.1289	0.0382	0.9156 (0.0016)

7. CONCLUSION

This study introduces a new three-parameter unit-bounded model, termed the Exponentiated Generalized Reduced Kies Distribution, which offers an improved alternative to several existing statistical distributions through applications to real-life datasets. Both graphical and numerical analyses demonstrate that the distribution's density can exhibit right-skewed, left-skewed, or symmetric shapes, while its hazard function may display either a bathtub or increasing failure rate. Key properties of the distribution are thoroughly explored. A comprehensive simulation study is conducted to evaluate and compare the performance of parameter estimators, revealing that the maximum likelihood estimation method generally outperforms the maximum product of spacings approach. To illustrate the practical relevance of the proposed model, it is applied to two real-life datasets. The findings suggest that this new distribution has strong potential as a flexible and effective modelling tool across various applied domains. For example, in medical studies, the EGRKiD could be applied to variables such as diagnostic test scores or proportions of affected tissue, which are bounded between 0 and 1 and may show either skewed or symmetric patterns. In finance, it could be used for modelling portfolio weight allocations, where capturing different shapes and tail behaviours is important for accurate risk evaluation. The EGRKiD's ability to adapt to these varied data structures gives it a practical advantage over other established unit-bounded distributions.

REFERENCES

[1] G. M. Cordeiro, E. M. Ortega, and D. C. da Cunha, "The Exponentiated Generalized Class of Distributions," J. Data Sci., vol. 11, no. 1, pp. 1–27, 2013. doi: https://doi.org/10.6339/JDS.2013.11(1).1086

[2] I. Elbatal and H. Z. Muhammed, "Exponentiated Generalized Inverse Weibull Distribution," Appl. Math. Sci., vol. 8, no. 81, pp. 3997–4012, 2014. doi: https://doi.org/10.12988/ams.2014.44256

[3] P. E. Oguntunde, O. A. Odetunmibi, and A. O. Adejumo, "On the Exponentiated Generalized Weibull Distribution," Indian J. Sci. Technol., vol. 8, no. 35, pp. 1–7, 2015. doi: https://doi.org/10.17485/ijst/2015/v8i35/85942

[4] H. M. Reyad et al., "The Exponentiated Generalized Topp Leone-G Family of Distributions," Pak. J. Stat. Oper. Res., vol. 15, no. 1, pp. 1–24, 2019. doi: https://doi.org/10.17485/ijst/2015/v8i35/85942

[5] M. El-Morshedy et al., "Exponentiated Generalized Inverse Flexible Weibull Distribution," Commun. Math. Stat., vol. 10, no. 3, pp. 413–434, 2021. doi I: https://doi.org/10.1007/s40304-021-00246-7

[6] N. Poonia and S. Azad, "A New Exponentiated Generalized Linear Exponential Distribution," Res. Math. Stat., vol. 8, no. 1, p. 1953233, 2021. doi: https://doi.org/10.1080/27658449.2021.1953233

[7] E. A. Elsherpienyi and E. M. Almetwally, "The Exponentiated Generalized Power Exponential Distribution," Pak. J. Stat. Oper. Res., vol. 18, no. 2, pp. 349–367, 2022. doi: https://doi.org/10.18187/pjsor.v18i2.3786

[8] L. B. S. Telee, M. Karki, and V. Kumar, "Exponentiated Generalized Exponential Geometric Distribution," Interdiscip. J. Manage. Soc. Sci., vol. 3, no. 2, pp. 37–60, 2022. doi: https://doi.org/10.3126/ijmss.v3i2.47862

[9] A. E. EL-Hady et al., "Discrete Exponentiated Generalized Family of Distributions," Comput. J. Math. Stat. Sci., vol. 2, no. 2, pp. 303–327, 2023. doi: https://doi.org/10.21608/cjmss.2023.203704.1014

[10] K. Keganne et al., "A New Extension of the Exponentiated Generalized-G Family," Sci. Afr., vol. 20, p. e01719, 2023. doi: https://doi.org/10.1016/j.sciaf.2023.e01719

[11] A. I. L. Abonongo and J. Abonongo, "Exponentiated Generalized Weibull Exponential Distribution," Comput. J. Math. Stat. Sci., vol. 3, no. 1, pp. 57–84, 2024. doi: https://doi.org/10.21608/cjmss.2024.275771.1059

[12] M. Kpangay, "On the Exponentiated Generalized Exponentiated Exponential Distribution," Int. J. Sci. Res. Eng. Dev., vol. 6, no. 1, pp. 941–951, 2023.

[13] Y. Altinisik and E. Çankaya, "Exponentiated Generalized Ramos-Louzada Distribution," Commun. Fac. Sci. Univ. Ankara Ser. A1 Math. Stat., vol. 73, no. 1, pp. 76–103, 2024. doi: https://doi.org/10.31801/cfsuasmas.1285065

[14] I. Sule et al., "A New Generalized Exponentiated Family," Reliab. Theory Appl., vol. 20, no. 1 (82), pp. 38–52, 2025.

[15] C. S. Kumar and S. H. S. Dharmaja, "On Reduced Kies Distribution," Collect. Recent Stat. Methods Appl., pp. 111–123, 2013.

[16] F. G. Akgül, "Comparison of Estimation Methods for Exponentiated Reduced Kies Distribution," Süleyman Demirel Univ. Fen Bilim.

Enstitüsü Derg., vol. 22, no. 3, pp. 1209–1216, 2018. doi: https://doi.org/10.19113/sdufbed.08036

[17] I. Usta and M. Akdede, "Bayesian Estimation of the Reduced Kies Distribution Parameters," Proc. Book, p. 138, 2019.

[18] C. S. Kumar and S. H. S. Dharmaja, "The Exponentiated Reduced Kies Distribution," Commun. Stat. Theory Methods, vol. 46, no. 17, pp. 8778–8790, 2017. doi: https://doi.org/10.1080/03610926.2016.1183786

[19] A. A. Al-Babtain et al., "A New Modified Kies Family," Math., vol. 8, no. 8, p. 1345, 2020. doi: https://doi.org/10.3390/math8081345

[20] M. A. Almuqrin et al., "A Flexible Extension of Reduced Kies Distribution," Complexity, vol. 2022, Article ID 6078567, 2022. doi: https://doi.org/10.1155/2022/6078567

[21] A. L. Bowley, Elements of Statistics, 6th ed. London: Staples Press, 1937.

[22] J. J. A. Moors, "A Quantile Alternative for Kurtosis," J. Roy. Stat. Soc. Ser. D (Statistician), vol. 37, no. 1, pp. 25–32, 1998. doi: https://doi.org/10.2307/2348376

[23] A. Z. Afify et al., "A New Unit Distribution," Electron. J. Appl. Stat. Anal., vol. 15, no. 2, pp. 460–484, 2022. doi: https://doi.org/10.1285/i20705948v15n2p460

[24] S. Nadarajah and S. Kotz, "Moments of Some J-Shaped Distributions," J. Appl. Stat., vol. 30, pp. 311–317, 2003. doi: https://doi.org/10.1080/0266476022000030272

[25] F. Sultana et al., "Parameter Estimation for the Kumaraswamy Distribution," Am. J. Math. Manage. Sci., vol. 37, no. 3, pp. 243–261, 2018. DOI: https://doi.org/10.1080/01966324.2018.1458166

[26] N. L. Johnson, S. Kotz, and N. Balakrishnan, Continuous Univariate Distributions, 2nd ed., vol. 2. Wiley, 1994.

[27] J. Mazucheli, A. F. B. Menezes, and M. E. Ghitany, "The Unit-Weibull Distribution," J. Appl. Probab. Stat., vol. 13, no. 2, pp. 1–22, 2018. doi: https://doi.org/10.1155/2018/2303796

[28] J. Mazucheli, A. F. B. Menezes, and S. Dey, "Unit-Gompertz Distribution," Statistica, vol. 79, no. 1, pp. 25–43, 2019 doi: https://doi.org/10.6092/issn.1973-2201/8497

[29] P. R. D. Marinho et al., "AdequacyModel: An R Package," PLoS One, vol. 14, no. 8, p. e0221487, 2019. doi: https://doi.org/10.1371/journal.pone.0221487

[30] R. Dasgupta, "On the Distribution of Burr," Sankhya B, vol. 73, pp. 1–19, 2011. doi: https://10.1007/s13571-011-0025-9

[31] R. A. ZeinEldin et al., "Different Estimation Methods for Type I Half-Logistic Topp–Leone Distribution," Math., vol. 7, no. 10, p. 985, 2019. doi: https://10.3390/math7100985